AD-A073 001 CALIFORNIA INST OF TECH PASADENA ARTHUR AMOS NOYES L--ETC F/G 7/4
SIMILARITIES AND DIFFERENCES BETWEEN ELECTRON AND PROTON TRANSF--ETC(U)
AUG 79 R A MARCUS N00014-79-C-0009
UNCLASSIFIED CONTRIB-6006 NL

| OF |
AD
A073001

END
DATE
FILMED
9-79
DDC

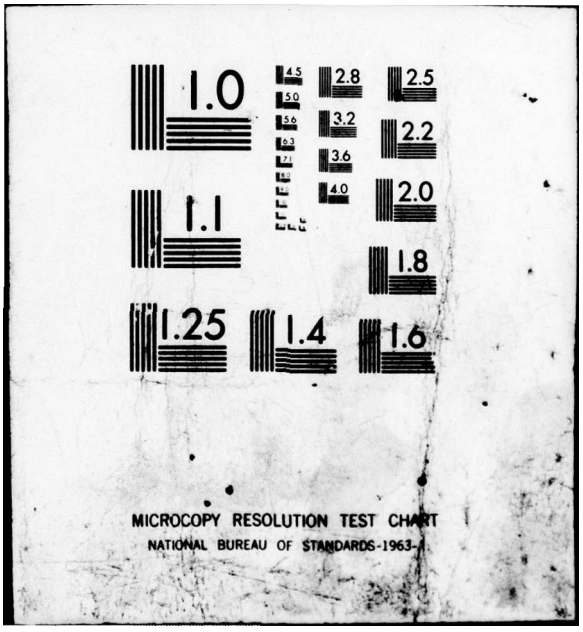
1.0
1.1
1.25
1.4
1.6
1.8
2.0
2.2
2.5
2.8
3.2
3.6
4.0
4.5
5.0
5.6
6.3
MICROCOPY RESOLUTION TEST CHART
NATIONAL BUREAU OF STANDARDS-1963-A

OFFICE OF NAVAL RESEARCH

Contract N00014-79-C-0009

Project NR 359-702

Technical Report No. 9

Similarities and Differences Between Electron and Proton Transfers at Electrodes and in Solution.

by R. A. Marcus

Prepared for publication in
the "Proceedings of the Symposium on Electrode Processes",
Electrochemical Society, 1979

CONTRIB-6006, TR-9

California Institute of Technology
Noyes Laboratory of Chemical Physics
Pasadena, California 91125

Aug[illegible]979

13 p.

R. A. Marcus
Principal Investigator

SIMILARITIES AND DIFFERENCES BETWEEN ELECTRON AND PROTON TRANSFERS AT ELECTRODES AND IN SOLUTION. THEORY OF A HYDROGEN OVERVOLTAGE REACTION.*†

R. A. Marcus

Arthur Amos Noyes Laboratory of Chemical Physics,
California Institute of Technology,
Pasadena, California 91125

Abstract

Depending on the initial energies, a proton transfer may proceed either via a saddle-point in a potential energy surface or by crossing from the reactants' to the products' valley before the saddle-point is reached. In the second path the analogy to weak-overlap electron transfers is pointed out. The present study is intended to unify previously divergent viewpoints, by showing how they are special cases of a more general picture. Expressions are obtained for the reaction rate in terms of the properties of the potential energy surface and of other properties of the system, using a hydrogen overvoltage reaction as an example.

*Contribution No. 6006.

†Supported by a contract from the Office of Naval Research.

Introduction

In a proton transfer, for example in the hydrogen overvoltage reaction (1) at an electrode M,

$$H_3O^+ + M(e) \rightarrow H_2O + H\text{-}M \qquad (1)$$

some dynamical effects result from the lightness of the H-particle, and several questions arise: Can a conventional transition state theory be used to calculate the reaction rate, with a transition state near some saddle-point region of the potential energy surface? Does the proton transfer occur so quickly that, as in weak-overlap electron transfers, a "nonequilibrium" solvent dielectric polarization arises?

Several authors[1-5] assume a conventional transition state for reaction (1) and also an equilibrium solvent dielectric polarization. Others[6] assume, instead, concepts analogous to those used in a weak-overlap electron transfer reaction, with its associated nonequilibrium polarization. Recently a unified treatment was outlined,[7] and a quantitative description is given in the present paper.

Potential Energy Surface and Reaction Paths

We first consider the potential energy surface for reaction (1) as a function of two of the coordinates, the H_2O-H and the H-M distances, using the usual[8] mass-weighted skewed axis coordinates (Fig. 1). There are also the bending motions of the O-H-M, the stretching motions of the other O-H stretches, and the coordinates of the solvent environment. The actual potential energy is a function of all of these coordinates. Path α in Fig. 1 is a path through the saddle-point, and path β is a path at any fixed O-M distance.

In the highly exothermic case, caused by a very favorable overpotential, a schematic diagram of the surface can resemble that in Fig. 2. Paths α and β are again drawn.

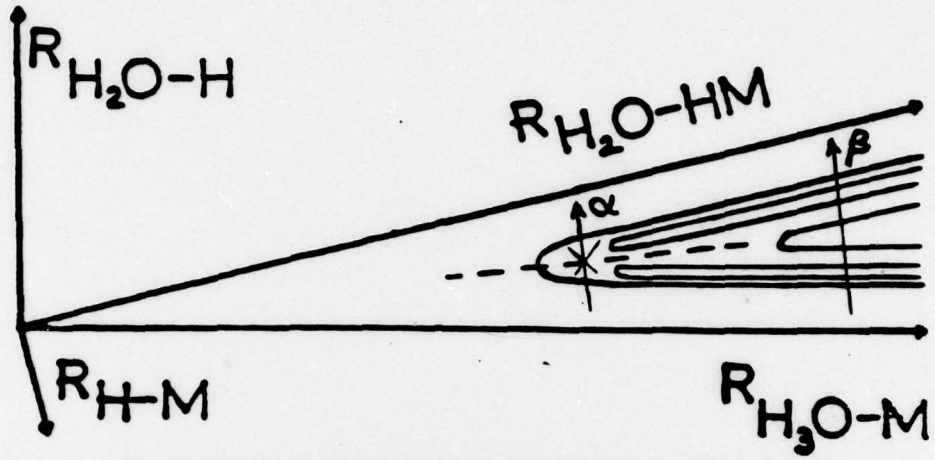

Fig. 1. Potential energy contour plot (schematic) for the three center reaction H_2O-H-M at a fixed value of the other coordinates and at a given metal-solution potential difference, for the case where the reaction is almost thermoneutral (symmetric). The rotated axes are scaled H_2O-HM and H-M distances (between O and the center of mass of HM and between H and M).[9] The configurations along the dashed line form the conventional transition state, and X denotes the saddle-point on the potential energy surface. Reaction paths α and β are described in the text.

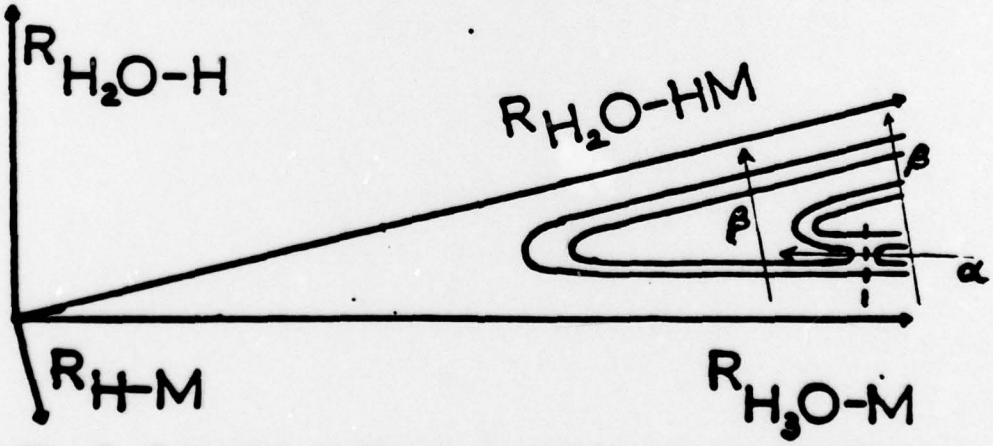

Fig. 2. Legend as in Fig. 1, but the reaction is now highly exothermic. The dashed line denotes the conventional transition state, passing through the saddle-point of the potential energy surface.

One task will be to decide whether the system ever reaches the saddle-point region as in path α in Fig. 1 or 2, or whether, either because the O-H vibrational energy is sufficiently high or because tunneling of the H from the O to the M may be large, the system moves from the reactants' valley to the products' valley before the saddle-point region is reached, as in path β in Fig. 1 and as in the β-path at a large O-M distance in Fig. 2.

Paths α and β can be competitive, conceivably one (α) prevailing in very exothermic or very endothermic conditions and the other (β) prevailing under more nearly thermoneutral conditions. A prescription for estimating the relative importance of the two paths is described in the present paper. Path β is assumed in Ref. 6 (but with a surface constructed from intersecting parabolas) and, in effect, path α is used in the usual transition state theory.

Energetics for Paths α and β

We shall be interested in introducing a relatively simple formalism which allows for these different reaction paths. To illustrate the approach, we use, for simplicity, a potential surface which treats changes in the O-H-M potential energy due to changes in O-H and H-M distances by a bond energy-bond order (BEBO) method,[4, 11] and which treats the remaining motions largely (though not necessarily entirely) in terms of their dielectric polarization behavior. In an approximation to BEBO, quite adequate where tested, the BEBO surface could be described by the expression[12]

$$V_e = n_2 \Delta V^0 + \Delta V' [n_1 \ell n\, n_1 + n_2 \ell n\, n_2]/\ell n\, 2 \ , \qquad (2)$$

where n_1 and n_2 are the bond orders of the H_2O-H and H-M bonds, respectively. At any point along the minimum potential energy path it is assumed[11, 12] that the sum $n_1 + n_2$ remains constant, namely unity. In Fig. 3 we have joined by a β-path any pair of points P and P′ lying on the minimum potential energy path, but in the reactants' and products' valleys, respectively. Eq. (2) can be replaced by a

more elaborate expression without changing the treatment below.

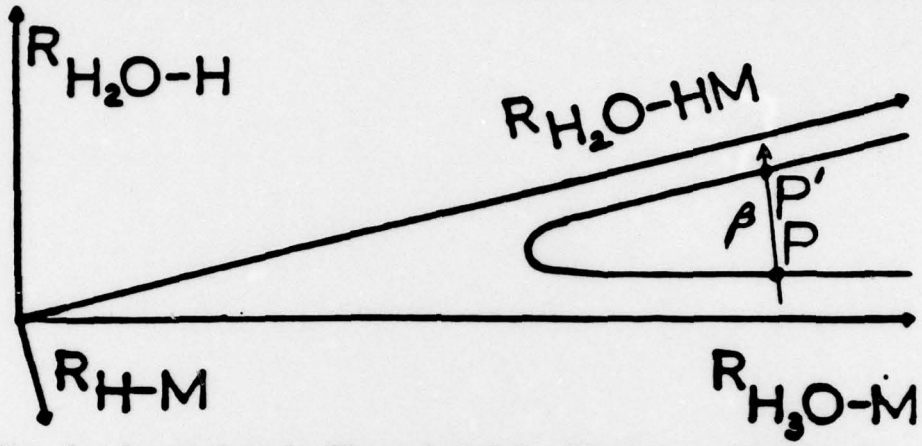

Fig. 3. Legend as in Figs. 1 and 2. The curve denotes the minimum potential energy path, which proceeds along the reactants' valley, over a saddle-point, and along the products' valley. The saddle-point may be situated as in Fig. 1 or as in Fig. 2 or, in the case of a very endothermic reaction, in the products' valley. Points P and P′ are corresponding pairs points which lie at the intersection of a β-path with the minimum potential energy path.

The difference of bond orders of the H-M bond at any pair of points P and P′ in Fig. 3 will be denoted by Δn,

$$\Delta n = n_2(P') - n_2(P) \quad . \tag{3}$$

Along each PP′ path the potential energy in Figs. 1-3 is given by Eq. (2) (with $n_1 + n_2 = 1$ at the points P and P′) and, along PP′, by Eq. (2) using bond length-bond order relations.

The interaction of the solvent with the $H_2O\text{-}H^+\text{-}M$ subsystem along the various paths is also to be included, and, for brevity and simplicity, we shall do so classically. (Various high frequency modes, treated structurally, could also be included and treated quantum mechanically.) We consider a particular value of the orientation-vibration polarization of the remaining coordinates $\underset{\sim}{P}_u(\underset{\sim}{r})$ at each point $\underset{\sim}{r}$ of the solvent medium.

An expression for the free energy of solvation of the reactants G^r_{sol} for any given $\underset{\sim}{P}_u(\underset{\sim}{r})$ function is[13]

$$G^r_{sol} = -(1 - D_{op}^{-1})\frac{1}{8\pi}\int \underset{\sim}{D}^r \cdot \underset{\sim}{D}^r \, d\underset{\sim}{r} - \int \underset{\sim}{P} \cdot \underset{\sim}{D}^r \, d\underset{\sim}{r} + 2\pi c \int \underset{\sim}{P} \cdot \underset{\sim}{P} \, d\underset{\sim}{r} \qquad (4)$$

where

$$\underset{\sim}{P} \equiv \underset{\sim}{P}_u / D_{op}, \qquad c^{-1} = \frac{1}{D_{op}} - \frac{1}{D_s} . \qquad (5)$$

D_{op} and D_s are the optical and static dielectric constants, and $\underset{\sim}{D}^r$ is is the electric field directly due to the charges. G^r_{sol} varies as the point P moves along the minimum potential energy curve in Fig. 3 since $\underset{\sim}{D}^r$ varies with position along that line. The first term in (4) is the solvation term when there is no orientation-vibration polarization $\underset{\sim}{P}_u$, the second term is a dipolar interaction of $\underset{\sim}{P}_u$ with the charges in a medium of dielectric constant D_{op}, and the last term is the orientation-vibration polarization energy stored up in the polarized dielectric; it vanishes when D_s equals D_{op}, as does $\underset{\sim}{P}_u$.

When the system in Fig. 3 is at the point P′ the solvation free energy is that of the products G^p_{sol} for the H_2O-H-M configuration P′. For the same $\underset{\sim}{P}_u$ it is given by the same expression as (4) but with r subscripts replaced by p's.

In the vicinity of P in Fig. 3 we let the system have a local H_2O-H-M protonic vibrational state of energy E^r_v, a solvation free energy G^r_{sol}, and an electronic energy V^r_e. The free energy of the system near P, $G^r(P)$, is then given by

$$G^r(P) = G^r_{sol} + E^r_v + V^r_e \quad . \qquad (6)$$

G^r_{sol} includes the electrode potential term since the $\underset{\sim}{D}$ in (4) includes fields due to charges on the electrode and in the ion atmosphere (double layer).

Energetics Alone a β-Path (Proton Jump)

When the system proceeds along a path β in Figs. 1-3, from

point P to point P′ (Fig. 3), it does so by a protonic motion so rapid that $\underset{\sim}{P}_u$ is constant along the PP′ path. With energy conserved during a protonic jump from the P to P′ valley, and with the entropy associated with the orientation-vibration polarization $\underset{\sim}{P}_u$ also unchanged during the transition at fixed $\underset{\sim}{P}_u$, we have

$$G^r(P) = G^p(P') \quad . \tag{7}$$

Thus far, the polarization $\underset{\sim}{P}_u$ in Eqs. (4)-(7) is arbitrary. As in electron transfer reactions we choose it so that G^r_{sol} is a minimum for a system at the point P, subject to the constraint imposed by (7). Thereby, one finds

$$\delta G^r = 0 = - \int (\underset{\sim}{D}^r - 4\pi c \, \underset{\sim}{P}) \cdot \delta \underset{\sim}{P}_u \, d\underset{\sim}{r} \tag{8}$$

$$\delta G^r - \delta G^p = 0 = - \int (\underset{\sim}{D}^r - \underset{\sim}{D}^p) \cdot \delta \underset{\sim}{P}_u \, d\underset{\sim}{r} \quad . \tag{9}$$

Multiplying the second equation by a Lagrange multiplier m, adding and setting the coefficient of $\delta \underset{\sim}{P}_u$ equal to zero, as the most general solution of (8) and (9), one finds at each point $\underset{\sim}{r}$ in the medium that

$$4\pi c \, \underset{\sim}{P}_u / D_{op} = (1 + m) \, \underset{\sim}{D}^r - m \, \underset{\sim}{D}^p \quad , \tag{10}$$

where D^r and D^p denote the electric fields for systems at P and at P′ in Fig. 3, directly due to the charges. The similarity of the procedure embodied in Eqs. (4), (8)-(10) to that used[14] for the transfer of another light particle, the electron, may be noted.

Introduction of this $\underset{\sim}{P}_u$ into (4) and into the corresponding expression for G^p_{sol} yields (11) and (14):

$$G^r_{sol} = G^r_{sol}\,(eq) + m^2\lambda \tag{11}$$

where the first term is the equilibrium solvation for a system at point P,

$$G^r_{sol}\,(eq) = -(1 - D_s^{-1}) \int \underset{\sim}{D}^r \cdot \underset{\sim}{D}^r \, d\underset{\sim}{r}/8\pi \tag{12}$$

and $m^2\lambda$ is the fluctuation term due to $\underset{\sim}{P}_u$'s being different from its equilibrium value in $G^r_{sol}(eq)$. λ is given by (13).

$$\lambda = \int (\underset{\sim}{D}^p - \underset{\sim}{D}^r) \cdot (\underset{\sim}{D}^p - \underset{\sim}{D}^r)\, d\underset{\sim}{r}/8\pi c \ . \tag{13}$$

The difference of charge distribution on the right hand side of (13) is expected to be roughly proportional to the Δn in Eq. (3), and so to depend on the point P. Similarly, the solvation for a system at point P′ in Fig. 3 is

$$G^p_{sol} = G^p_{sol}(eq) + (m+1)^2\lambda \ . \tag{14}$$

The value of m is determined from (7), (11), and (14):

$$-(2m+1)\lambda = G^p_{sol}(eq) - G^r_{sol}(eq) + E^p_v - E^r_{v'} + V^p_e - V^r_e \tag{15}$$

when the system near point P in a given vibrational state v of energy E^r_v, is transformed by the proton jump into a system near P′ in a proton vibrational state v′ of energy $E^p_{v'}$.

Rate Expression for the β-Path

We denote by $\kappa_{vv'}(E^0_t)$ the probability of a reactive $v \rightarrow v'$ protonic transition, when the initial translational energy along the line of centers in Figs. 1-3 is E^0_t and the initial protonic vibrational energy is E^0_v. The transition state expression for the reaction rate is given by [15]

$$k_{rate} = \sum_{v,v'} \int_{E^0_t=0}^{\infty} \kappa_{vv'}(E^0_t)\, e^{-(E^0_v + E^0_t)/kT}\, dE^0_t\, f/Q_v\, kT \tag{16}$$

where

$$f = \frac{kT}{h}\, e^{-(\Delta G^r_{sol} + m^2\lambda)/kT}\, \frac{(2\pi\mu kT)}{h^2}\, \frac{1}{(2\pi\mu kT)^{3/2}/h^3} \ ,$$

$$= Z\, e^{-(\Delta G^r_{sol} + m^2\lambda)/kT} \ . \tag{17}$$

ΔG^r_{sol} is the increment in equilibrium solvation free energy on going from ∞ to P. In (17) the translational partition function for the three translational degrees of freedom of the reactant, and that for a delocalized reactant on the surface were introduced. (Corrections for localized adsorption can be added but are omitted in (16)-(17) for brevity.) Q_v is the protonic vibrational partition function for the reactant in Figs. 1-3, and Z is the collision frequency $(kT/2\pi\mu)^{1/2}$ for collisions with unit area of the electrode.

The calculation of $\kappa_{vv'}$ proceeds as follows: One first locates the point P of deepest O-M penetration, namely where the translational energy along the O-M direction vanishes, i.e., where, in the reactants' valley we have, in this β-path mechanism,

$$E^0_v + E^0_t = E^r_v + \Delta V^r_e \tag{18}$$

E^r_v and ΔV^r_e refer to the protonic vibrational energy and the increment in potential energy (from the H_3O^+ moving from ∞) at point P in Fig. 3. In calculating E^r_v the vibrational quantum number v is taken as constant (v) within the reactants' valley (adiabatic treatment for the H-vibration in the valley). E_v differs from E^0_v only because of changes in cross-sectional profile (e.g., in vibration frequency) during motion along that valley of the potential energy surface.

If the value of E^r_v at P is sufficiently large to overcome any V_e barrier from reactants to products along the β-path at that P, the corresponding $\kappa_{vv'}$ is set equal to unity. Otherwise, a tunneling calculation for $\kappa_{vv'}$ is used. Recently, a useful calculation which includes tunneling along a β-path and, where necessary, initially along an O-M coordinate was given in Ref. 10 and could be used for the present purpose.

The barrier along this β-path is modified somewhat by the presence of the G_{sol} term for the cited $\underset{\sim}{P}_u$. Thus, changes in $V_e + G_{sol}$ along this β-path serve as the effective barrier to proton motion

along that path (Appendix).

Thus far, the electrode-solution potential difference φ has not been specifically introduced. It is implicitly present in each G_{sol} terms. By evaluating these terms one obtains φ. As in electron transfer theory,[16] a "standard potential" φ^0 for reaction (1) in the prevailing medium can also be introduced by setting the free energy of activation terms ΔG^r and ΔG^p equal at that φ. One can then express the rate of the forward reaction in terms of the difference $\varphi - \varphi^0$.

Decision as to Paths α and β

If for any point P for any given E_v^0 and E_t^0 in Eq. (16) the point P is closer to the origin than the saddle-point, then path α will dominate rather than path β for that (E_v^0, E_t^0) pair. If point P, in the case of Fig. 1, is quite close to the saddle-point, the Δn defined by (3) becomes very small and so the term $D^r - D^p$ arising from a difference in charge distributions at P and $\tilde{P}'$ also becomes small, and so does, thereby, the λ in Eq. (13). Thus, with this approximate vanishing of the $m^2\lambda$ in (17) one has again retrieved the usual transition state theory result. On the other hand, when the barrier along a β-path can more easily be overcome, either by excess vibrational energy in E_v^r or by a sufficiently large value of $\kappa_{vv'}$, one obtains a β-path mechanism rather than one proceeding via the saddle-point in the potential energy surface.

The above remarks also serve to point out the similarities and differences between proton transfers and weak-overlap electron transfers. The weak-overlap electron transfer proceeds via the counterpart of a β-path, and has the $m^2\lambda$ terms of the previous section. The proton transfer can proceed via an α-path, wherein the $m^2\lambda$ is absent, or via a β-path, depending on the initial conditions. The remarks made earlier on the hydrogen overvoltage reaction are also intended to apply to other (e. g., homogeneous

proton transfers.

Appendix: Variation in $\underset{\sim}{D}$ Along a β-Path

$\underset{\sim}{D}$ varies along a β-path, since the electronic structure of the system varies along that path. $\underset{\sim}{D}(\underset{\sim}{r})$ is equal to (cf Eq. (5.4) of Ref. 13)

$$\underset{\sim}{D}(\underset{\sim}{r}) = -\nabla_{\underset{\sim}{r}} \int |\psi(\underset{\sim}{r}_j)|^2 \sum_i \frac{e_i}{|\underset{\sim}{r} - \underset{\sim}{r}_i|} \prod_j d\underset{\sim}{r}_j + C \qquad \text{(A1)}$$

where ψ is the electronic wavefunction for any nuclear configuration, and is a function of the coordinates of all electrons j of the reactants, and the sum is over all i, i.e., over all electronic and nuclear charges e_i in positions $\underset{\sim}{r}_i$. Thus, this $\underset{\sim}{D}(r)$ can be calculated from an electronic structure calculation. The C in (A1) is the contribution to $\underset{\sim}{D}$ arising from the other charges on the electrode and from the ion atmosphere (including double layer).

References

1. cf review by A. J. Appleby, J. O'M. Bockris, R. V. Sen, and B. E. Conway, MTP Internat. Rev. Sci. Phys. Chem. Ser. 6, 1 (1973).

2. J. O'M. Bockris, S. Srinivasan, and D. B. Mathews, Disc. Faraday Soc., 39, 239 (1965).

3. B. E. Conway and M. Solomon, Ber. Bunsenges. Phys. Chem., 68, 331 (1964); M. Solomon and B. E. Conway, Disc. Faraday Soc., 39, 223 (1965).

4. M. Solomon, C. Enke, and B. E. Conway, J. Chem. Phys., 43, 3989 (1965).

5. S. G. Christov, J. Res. Inst. Catal. Hokkaido Univ., 16, 169 (1968).

6. E.g., R. R. Dogonadze, A. M. Kuznetsov, and V. G. Levich, Electrochim. Acta, 13, 1025 (1968).

7. R. A. Marcus, Physicochem. Hydrodyn. (Levich Conf.), 1, 473 (1977).

8. S. Glasstone, K. J. Laidler, and H. Eyring. "The Theory of Rate Processes" (McGraw-Hill, New York, 1941), Chap. 3.

9. The H_2O mass is taken as concentrated on the O, in the scaling, and the M mass is taken as infinite.

10. M. Ya. Ovchinmikova, Chem. Phys., 36, 85 (1979).

11. H. S. Johnston. "Gas Phase Reaction Rate Theory" (Ronald Press, New York, 1966).

12. R. A. Marcus, J. Phys. Chem., 72, 891 (1968).

13. R. A. Marcus, Faraday Symp. Chem. Soc., 10, 60 (1975). For clarity, dielectric image effects are neglected, by using (4) instead of the expression in Ref. 14 below.

14. R. A. Marcus, J. Chem. Phys., 24, 966 (1956).

15. cf also R. A. Marcus, J. Chem. Phys., 43, 1598 (1965), Eq.(14).

16. E.g., R. A. Marcus. In "Special Topics in Electrochemistry" P. A. Rock, ed. (Elsevier, Amsterdam, 1977), p. 180 (ONR Technical Report No. 12, 1957).